Energy-resolved angular distributions and the population partition of excited state Rh atoms ejected from ion bombarded Rh {001}

Chun He, Z. Postawa,[a] M. El-Maazawi, S. Rosencrance, B. J. Garrison, and N. Winograd
Department of Chemistry, The Pennsylvania State University, University Park, Pennsylvania 16802

(Received 12 April 1994; accepted 14 June 1994)

The energy-resolved angular distributions of Rh atoms ejected from Rh {001} by bombardment with 5.0 keV Ar^+ ions have been measured for the ground state ($a\ ^4F_{9/2}$) and the two lowest lying excited state ($a\ ^4F_{7/2}$,$a\ ^4F_{5/2}$). Simultaneous measurements on these electronic states provide us an opportunity to examine the influence of electronic interactions on desorbed particles. The experimental results show that there is a sequential variation in the angular distributions as the excitation energy increases. These variations are attributed to the interaction between the substrate electrons and the excited state atom as it is being ejected from the surface. Since the measurements are performed using multiphoton ionization via a single intermediate state, the population partition among the three lowest states is obtained as well. The excitation probabilities of the $a\ ^4F_{7/2}$ and $a\ ^4F_{5/2}$ states are compared with those predicted from the expression $\exp(-A/av_\perp)$ and with a recently proposed model involving interatomic collisions above the surface. Results suggest that atoms excited via this mechanism make a significant contribution to the population of atoms ejected with low ejection velocities for the first-excited $a\ ^4F_{7/2}$ state (0.19 eV), as reported previously. Moreover, we suggest that an even higher proportion of atoms in the $a\ ^4F_{5/2}$ state are produced via this mechanism.

I. INTRODUCTION

The interaction of energetic particles with solids initiates a complex dynamical chain of events, including atomic motion, electronic excitation, and desorption of atomic and molecular species.[1] The atomic motion has been successfully modeled for atoms in their ground electronic state using molecular dynamics computer simulations.[2–7] This modeling provides a reasonably accurate description of the velocity and angular distributions of the ejected particles,[2,4,6,7] as well as qualitative information about lattice damage subsequent to ion bombardment.[8–10]

Therre have been a number of attempts to describe the electronic excitations that occur in concert with the nuclear motion.[11–15] These models generally separate the excitation process from the de-excitation or relaxation process to allow prediction of the final yield of electronic states. The initial step has been described using a statistical model based on excitation via inelastic energy transfer to a target atom. The relaxation process has been predicted to vary exponentially with the reciprocal of velocity as

$$\exp(-A/av_\perp), \tag{1}$$

where A and a are constants and $v_\perp$ is the component of velocity normal to the surface.[13–15] This expression has been a good representation of a number of experimental investigations although deviations at lower velocities have been observed.[16–19]

Recently, we have been interested in measuring the population of various excited states of atoms ejected from single crystals as a function of their kinetic energy and takeoff angle. It is hoped that this approach will yield more insight into the elucidation of excitation mechanisms than the corresponding integrated quantities. In our experiments, we have obtained these distributions for Rh atoms desorbed from a clean Rh {001} target in their ground electronic state ($a\ ^4F_{9/2}$) and their first excited state ($a\ ^4F_{7/2}$). The $a\ ^4F_{7/2}$ state, metastable with respect to decay, is part of the ground state manifold of fine structure states and lies 1530 cm^{-1} (0.19 eV) above the $a\ ^4F_{9/2}$ state. The experiments were made possible with a special energy and angle-resolved detection scheme which employs resonance ionization spectroscopy to determine the population of each state.[18,19]

Interpretation of these results is based on a model which combines molecular dynamics computer simulations of the ion impact even to describe classical motion and collision-induced excitation to describe inelastic effects.[19–25] This approach is useful since the computer modeling is known to yield a reasonably accurate account of the motion of atoms in their ground state.[2,4,6,7] When two of these atoms experience a close interaction, there is assumed to be a certain probability of excitation. The atom is then allowed to experience a time-dependent decay as it travels through the solid, through the interface and into the vacuum. This approach has been successful in helping to elucidate the behavior of the experimental results found for the population of the $a\ ^4F_{7/2}$ state of Rh desorbed from Rh {001}.[19,23,24] For this case, there is an exponential dependence of excitation probability on $v_\perp$ with deviations found at low velocity ($\lesssim$10 eV). These deviations arise from (i) surface binding energy effects,[26–28] (ii) blocking and channeling effects in the surface layer, especially at high takeoff angles,[28] and (iii) re-excitation due to collisions above the surface.[19,23–25] This latter phenomenon is particularly interesting since it provides a new mechanism of inelastic excitations. Under the proper circumstances, it can be an effective mechanism of energy transfer since the excitations are long-lived, especially if the electronic excited

[a]Present address: Institute of Physics, Jagellonian University, 30-549 Krakow, Poland.

 0021-9606/94/101(7)/6226/7/$6.00 © 1994 American Institute of Physics

states are metastable in character. Typically, this type of collision occurs 1–20 Å above the crystal surface. It is a particularly interesting mechanism since its influence dominates the excitation probability after the contribution from other excitation mechanisms have become negligible. It may also play a role in ionization, especially for those systems which exhibit low ionization probabilities.

In this paper, we examine the behavior of the second electronic state of Rh ($a\ ^4F_{5/2}$) desorbed from Rh {001} and compare this behavior to that found previously for the $a\ ^4F_{7/2}$ level. This $a\ ^4F_{5/2}$ level, like $a\ ^4F_{7/2}$, is metastable with respect to decay, is part of the ground state manifold, and lies 2598 cm^{-1} (0.32 eV) above the $^4F_{9/2}$ state.[29] This situation allows a detailed study of the role of the magnitude of the excitation energy in determining the excitation probability using energy levels with very similar electronic character. Our results show that the intensity of the $^4F_{5/2}$ state is 30 times smaller than for the $a\ ^4F_{7/2}$ level and is nearly independent of velocity at kinetic energies less than 50 eV. The results are consistent with our previously developed collision-induced excitation model. The unusual velocity dependence is understood within the framework of the theory as originating from collisions over the crystal surface. This excitation mechanism dominates others for the $a\ ^4F_{5/2}$ level since the initial excitation probability is low and the excitations that occur within the solid and at the surface are almost completely quenched by the time desorption occurs. The results imply the electronic levels should not necessarily exhibit Boltzmann population distributions[30] and suggest that collisions over the surface can be a dominant pathway for inelastic excitations.

II. EXPERIMENTAL ARRANGEMENT

Experimental details and the procedure for obtaining energy-resolved angular distributions have been presented previously,[31] so only the essential features and modifications will be summarized here. As shown in Fig. 1, the system consists of an ultrahigh vacuum chamber with a base pressure of 1×10^{-10} Torr equipped for low-energy electron diffraction (LEED) and Auger electron spectroscopy (AES). An Ar^+ ion source is provided by an Ar gas ion gun capable of operating either in a continuous mode for *in situ* crystal cleaning or in a pulsed mode for performing experiments. The Ar^+ ion is accelerated to 5 keV and then mass selected via a magnetic sector to eliminate any impurities from the Ar gas (99.9995% purity) and from the interior of the ion source. The Rh sample of 99.99% purity is oriented to within ±0.5° of the {001} face by Laue back reflection. The cleaning procedure involves many cycles of ion bombardment (6 $\mu A/cm^2$, 30 min) and annealing (930 K, 20 min). A final flash to 1400 K results in a bright, sharp (1×1) LEED pattern.

Desorbed neutral Rh atoms are selectively ionized by multiphoton resonance ionization. As illustrated in Fig. 2, the ionization schemes used in the present investigation involve a one-photon excitation of Rh atoms from $a\ ^4F_J$ ($J=9/2$, 7/2, and 5/2) to the $z\ ^2F^0_{7/2}$ level (3.97 eV) followed by subsequent ionization via absorption of a second photon. The excitation and ionization photons originate from a frequency-doubled, tunable dye laser, pumped by the second harmonic of a Nd:YAG laser and are focused into a $1\times10\ mm^2$ ribbon shape. The ionization zone created by this ribbon-shaped laser beam is large enough to cover particles ejected at differ-

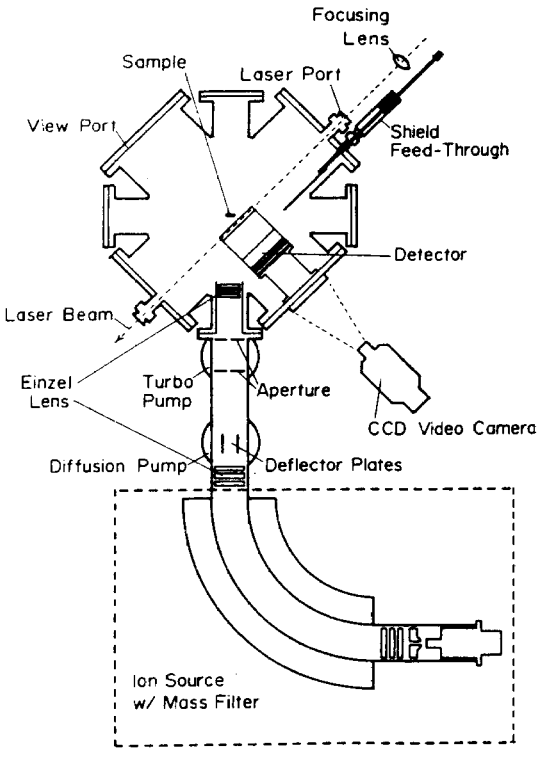

FIG. 1. Schematic representation of the experimental setup used to measure the state-, angle-, and kinetic energy-distribution of neutrals desorbed from ion bombarded surfaces.

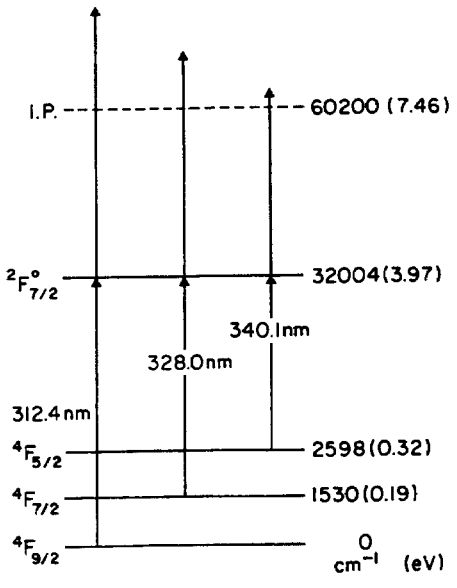

FIG. 2. Multiphoton resonance ionization scheme used to detect the Rh atoms in the ground ($a\ ^4F_{9/2}$), first-excited ($a\ ^4F_{7/2}$), and the second-excited ($a\ ^4F_{5/2}$) states.

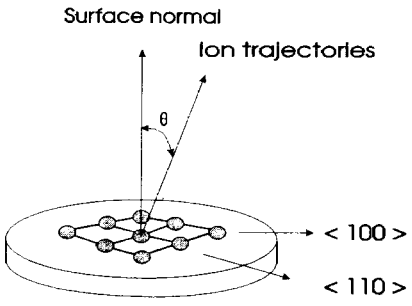

FIG. 3. Schematic representation of Rh {001} crystal face with open surface direction of ⟨100⟩ and close-packed direction ⟨110⟩ azimuthal directions shown. A polar angle of $\theta = 0°$ corresponds to surface normal and a polar angle $\theta = 90°$ corresponds to grazing angle.

ent polar-angles (0°–90°) with a fixed azimuthal angle resolution (±1.0°). Energy-resolved angular distributions at different azimuthal angles are obtained by rotation of the manipulator while monitoring the LEED pattern of the single crystal. While the resonant absorption frequencies of the ground ($a\ ^4F_{9/2}$) and first-excited ($a\ ^4F_{7/2}$) states to the intermediate state are accessible with the second harmonic of DCM dye, the transition of the second-excited state ($a\ ^4F_{5/2}$) to the intermediate requires the use of LDS-698 dye.

Energy-resolved polar angle distributions were obtained in the range of $\theta = 0°$ (normal ejection) to $\theta = 90°$ (grazing angle ejection) using ion extraction optics and a 75 mm diameter chevron multichannel plate (MCP). Angle definitions are shown in Fig. 3. Kinetic energy resolution was achieved by a combination of velocity time-of-flight and mass time-of-flight spectrometers. The data acquisition sequence is as follows: a 250 ns pulse of 5 keV Ar^+ ion is focused onto a 2 mm diam spot normal to the Rh {001} sample. Upon impact of the ion pulse, an ion extraction field is activated to reject charged particles. A 6 ns laser pulse with variable power of 0.1–2 mJ is positioned 1.5 cm above the impact center with a 45° angle between the sample surface and the ribbon-shaped laser beam. The tunable ultraviolet (UV) laser beam selectively ionizes a portion of the free-flying neutral atoms in a specific quantum state at a time delay (τ_E) after the ion-pulse impact, thus defining the time-of-flight. By varying the time delay between the ion beam pulse and the laser pulse a time-of-flight measurement, velocity-revolved data in the range of 0–50 eV of desorbed neutral atoms are obtained. The ionized particles, then accelerated by an extraction field, arrive at the front of the microchannel plate assembly at time τ_M, and illuminate a phosphor screen behind the MCP assembly. The time τ_M is governed by the mass-to-charge ratio of the ion of interest. The image is recorded by a CCD camera placed behind the phosphor screen.

After acquisition of the image, a set of intensity maps, each corresponding to a different delay time is stored in a laboratory computer. A software program is used to deconvolute the kinetic energy and angular information, providing separately resolved kinetic energy and polar angle distributions. By varying the laser frequency and the azimuthal angle of the sample, it is possible to determine the velocity distribution, spatial distribution, and relative population of ejected Rh atoms in each of the specified quantum states. The kinetic energy resolution is ±4% for 5 eV particles and ±15% for 50 eV particles while the polar angle resolution is ±2.5°. This resolution is adequate since the energy and spatial distributions are not rapidly changing for sputtered particles. Typically, in a 3 min run, 1×10^{12} ions/cm^2 are incident on the sample which is sufficient to collect a kinetic energy- and angle-resolved map. This leads to erosion of less than 0.5% of a monolayer and assures negligible surface damage by the incident ion beam.

III. RESULTS AND DISCUSSION

In this section we first examine the population of sputtered Rh atoms in the ground, first-excited, and second-excited states as determined from photoion intensity maps. In the second part of this section, we report the energy and angular distributions of each of these states, pointing out obvious common features as well as differences. Finally, these results are compared to predictions of a molecular dynamics computer simulation which incorporates electronic excitations into its basis. The comparison suggests that excited states formed by collisions between atoms that are above the surface are more important for the second excited state than for the first excited state.

A. Population partition

In order to obtain the population distribution of sputtered Rh atoms in the three lowest electronic states, one must determine the relationship between the signal intensity and the number of atoms sputtered from a surface. For the resonant excitation step, it is necessary to know the integrated excitation probability, degeneracies of the lower and upper states, as well as the photon fluence produced by the laser itself. Although transition probabilities, or branching ratios, for Rh atoms are well-known,[32] these coefficients were obtained under weak flux field conditions, i.e., under the assumption that the number density of atoms excited from the lower or initial state to the upper state is much smaller than the total number density of atoms in the initial state. In the present experiment, the flux generated by the 6 ns UV pulse laser is very high and reaches the condition of strong saturation. The relationship between the laser-induced signal intensity and the number density of the absorbing species has been shown to be straightforward when strong saturation is achieved for the excitation channel.[33] The relative excitation probability is then simply proportional to g_u/g_i, where the g_u and g_i are the statistical weights of the upper and initial (lower) states involved in the transition.

For the ionization step, the primary factor is the ionization cross section which couples the excited state to the continuum above the ionization limit. This transition probability is a function of state, photon flux density, and laser frequency. In most cases the ionization cross section is unknown. In the present work, strong saturation occurs in the resonant excitation though not in the subsequent ionization step. When a single fine-structure state is chosen, the ionization cross section can be assumed to be constant provided that the laser frequencies which produce the resonant transi-

tions for the ground and excited state are at least a few nm away from autoionizing states. The correlation between state population N_i and detected photoion intensity I_i ($i = a\ ^4F_{9/2}, a\ ^4F_{7/2}$ or $a\ ^4F_{5/2}$) can be expressed as

$$I_i = CN_i g_u / g_i P, \tag{2}$$

where C is a proportionality constant and P is the laser power. The photoion intensities for the ground and excited states used in the above expression were obtained by integrating the angle- and energy-resolved intensity map for each state along the ⟨110⟩ and ⟨100⟩ directions of Rh {001} and then adding these integrals together. For each of the three excitation schemes shown in Fig. 2 a laser power-dependence study was performed between 0.1–6 mJ and a least-square-fit was made for the linear portion of the power-dependence curves. The fitting parameters were then used to correlate the photoion intensities between these transitions for the power region where linear portions of the three curves overlap. The relative population ratios found through the above data evaluation procedure are 1.0 for $a\ ^4F_{9/2}$, 0.26 for $a\ ^4F_{7/2}$ and 0.0087 for $a\ ^4F_{5/2}$. Information concerning the population of the third excited state, $a\ ^4F_{3/2}$, is not yet available because allowed transitions to the intermediate state are either inaccessible to our available laser wavelengths or are overlapped with other transitions involving the first excited state.

B. Energy-resolved angular distributions of Rh in excited states

The polar angle distributions for the ground ($a\ ^4F_{9/2}$), first excited ($a\ ^4F_{7/2}$), and second excited ($a\ ^4F_{5/2}$) states of Rh atoms ejected from Rh {001} as a function of kinetic energy are shown in Fig. 4. In Fig. 4 the left side of the figure reports distributions obtained along the ⟨110⟩ azimuth, while the right side of the figure shows distributions obtained along the ⟨100⟩ azimuth. The data for all three states exhibit a number of similarities. The yields are higher along the open ⟨100⟩ azimuthal direction than along the close-packed ⟨110⟩ direction. the most intense peak is at $\theta = 42°–48°$ along the ⟨100⟩ direction followed by the peak at $\theta = 30°–34°$ along the ⟨110⟩ direction. There are hints of an additional peak in the direction normal to the surface, $\theta = 0°$. There is almost no intensity at grazing angles especially in the ⟨110⟩ direction. It is also apparent that the polar angle distribution depends on the kinetic energy of the sputtered atom, particularly along the ⟨100⟩ azimuth. The amount of normal ejection relative to the amount of off-normal ejection increases as the kinetic energy increases.

The data also reveal systematic variations in the angular distributions of ejected atoms among the ground state, the first excited state and the second excited state. First, the off-normal peak in the excited state distribution occurs closer to the surface normal than in the ground state distribution. For example, for particles ejected along the ⟨100⟩ crystallographic direction with kinetic energies between 5–10 eV, the maxima for the first- and second-excited states peak at 43.6° and 41.2°, respectively, compared to that found for the ground state at 47.5°. A similar trend is observed for the ⟨110⟩ direction. Secondly, there is a gradual increase in the amount of normal ejection in comparison to that of the off-normal signals. However, as the kinetic energy of the ejected particles increases, these trends become less pronounced. Another important observation is that all of the above-mentioned features depend strongly on the crystallographic direction at which the data are collected. Finally, in general, the off-normal peaks are less intense relative to the intensity in the normal direction.

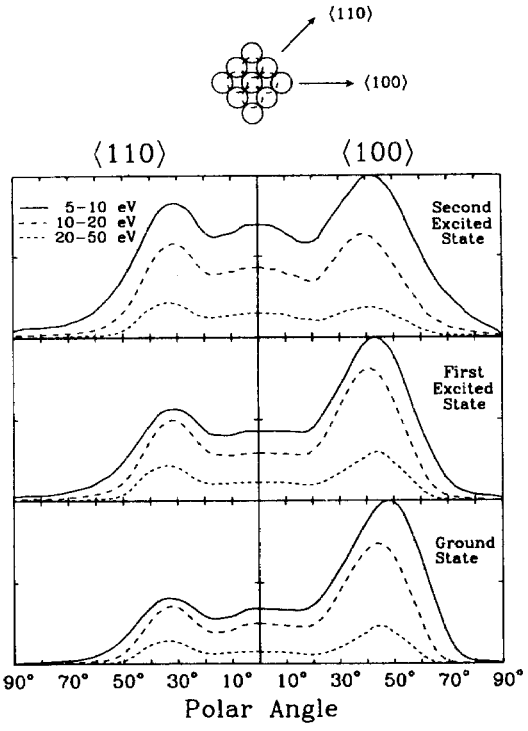

FIG. 4. Polar angle distributions of sputtered Rh atoms in the ground, first-excited, and second-excited states at fixed kinetic energy ranges (5–10 eV, 10–20 eV, and 20–50 eV). The data along the azimuthal directions ⟨110⟩ and ⟨100⟩ are presented in the first and second columns, respectively. In each frame the data are normalized to the peak intensity of the curve which corresponds to kinetic energy 5–10 eV along the azimuthal direction ⟨100⟩.

C. Excitation probabilities of the $a\ ^4F_{7/2}$ and $a\ ^4F_{5/2}$ excited states

The energy and angle resolved data for all three states are presented in Fig. 5 and from these data information about the population of atoms ejected with a specific velocity, angle and electronic state can be obtained. In general, a ratio of the number of excited state atoms to ground state atoms is a quantity of theoretical significance. For example, the molecular dynamics simulations yield $N_i(v, \theta, \phi)$ where N_t is the total number of ejected atoms. The probability to excite an atom to state i is then

$$P_i(v, \theta, \phi) = N_i(v, \theta, \phi) / N_t(v, \theta, \phi). \tag{3}$$

For our system where $P_i \ll 1$, we have assumed that the populations may be directly examined from the ratio[19,23,24]

$$N_i(v, \theta, \phi) / N_g(v_1, \theta, \phi)$$

or

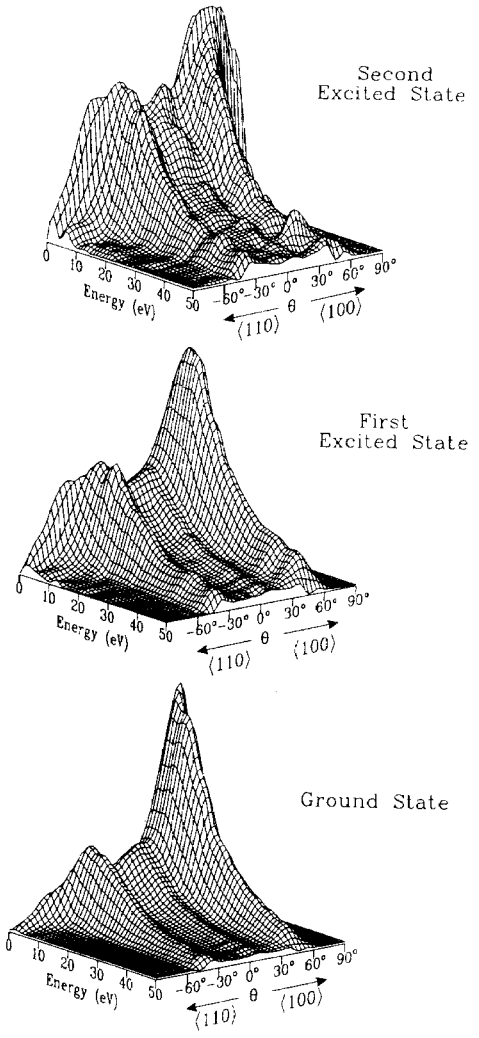

FIG. 5. Energy- and angle-resolved intensity maps for the $a\ ^4F_{9/2}$ ground and the $a\ ^4F_{7/2}$,$a\ ^4F_{5/2}$ excited states of Rh atoms ejected from Rh {001}. The plots are normalized to the highest intensity in all three cases. The polar angle θ is measured with respect to the surface normal.

$$(dN_i/dv)/(dN_g/dv), \tag{4}$$

where N_g is the number of atoms ejected in the ground electronic state. This representation of the data are given in Figs. 6(a) and 6(b) for both excited states. The probabilities are computed using all particles with $20°<\theta<30°$ and for two principal azimuthal directions of Rh {001}. As suggested from the form of Eq. (1), the probabilities are plotted on a log scale as a function of $1/v_\perp$.

The behavior of these data are quite unexpected. As we have already noted, the log of first excited state population follows the predicted $1/v_\perp$ dependence at high velocity, but levels off to become nearly independent of velocity or low velocities. The second excited state, however, shows almost no velocity dependence over the measured range of 0–50 eV. These results suggest that there are very different mechanisms at work and that the survival probabilities may not be well described by a simple Boltzmann-type approximation.[30]

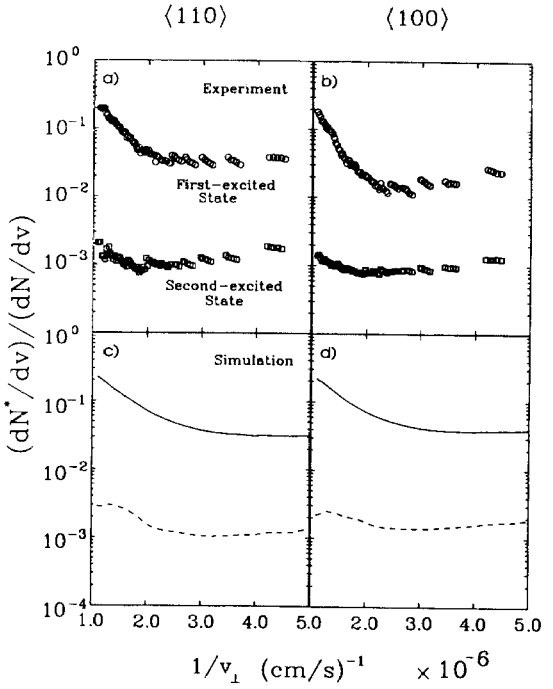

FIG. 6. Ratios of the number density of the first-excited state (upper curve) and the second-excited state over that of the ground state, $(dN^*/dv)/(dN/dv)$, vs $1/v_\perp$. (a) and (b) are experimental results for ejection along ⟨110⟩ and ⟨100⟩ azimuthal directions. The corresponding results from the computer simulations are shown in (c) and (d).

To begin to understand these data, we have examined the implications of a collision-induced excitation model described in detail in a series of previous papers.[19,23–25] Briefly, with this model the classical motion of Rh atoms after bombardment is described using a molecular dynamics computer simulation performed with an embedded atom (EAM) potential.[2] This calculation provides time-dependent information about any collisions that may occur during the atom ejection process. If a collision is found to occur, we assume a velocity-dependent excitation probability $P(v)$ as

$$P(v)=P^0(v)R(v), \tag{5}$$

where $P^0(v)$ is the initial value of the excitation probability at the time of collision and $R(v)$ is the survival probability of the excited atom as it traverses the solid. The excitation process is assumed to occur when the encounter distance between two atoms is smaller than a critical threshold distance, r_{th}. The decay rate is influenced by an environment-dependent lifetime. Although there are a number of parameters here, previous calculations have utilized values either selected from *ab initio* electronic structure calculations or fit from experimental data.

Results of these calculations have been shown to be in excellent agreement with experimental measurements of the velocity and angle dependence of N^*/N for the first excited state of Rh.[23,24] The results show that the part of the curve that is logarithmically dependent on $1/v_\perp$ is easily explained by a simple Hagstrom de-excitation model.[13–15] The low velocity portion of the curve arises from surface binding energy

effects, from blocking and channeling effects in the surface layer and from collisions over the surface. The observation that collisions over the surface may lead to a measurable degree of electronic excitation is particularly interesting, since this mechanism may be dominant for systems where the excitation probability is small. These collisions may also contribute to ionization, although such mechanisms have not yet been proposed.

A quantitative investigation of the events which give rise to collisions above the surface is difficult to extract due to their infrequent occurrence in the molecular dynamics calculations. Bernardo and Garrison[25] have employed a statistical approach whereby the angular distributions, energy distributions, surface position and ejection times were parametrized so they could be used to predict the probable fate of any given surface atom. With their model, an initial set of these values are assigned to two arbitrary particles which are then allowed to eject. Using a Rh dimer potential, the distance of closest approach may be quickly calculated for a large set of atoms. If this distance is found to be closer than r_{th} and the collision is found to occur above a certain minimum height over the surface (1.5 Å), then excitation with the initial probability P^0 is assumed to have occurred. Value for r_{th} of 1.85 Å and P^0 of 0.76 were found to reproduce the experimental data. The behavior of particles excited at the surface is fit to an exponential relation and combined with those found to collide over the surface to yield the total excitation probability curve. This approach accounts for many of the variations of the excitation probability as a function of velocity and angle, and illustrates the importance of collisions over the surface as a process for producing the majority of excited atoms at low velocities.

Can this model be extended to predict the behavior of the second excited state of Rh? At this stage, there are many unknown parameters and the possibility of making an *a prioir* calculation is not feasible. It is feasible, however, to compare the probability of collisions over the surface as a function of the magnitude of the collision energy. This would seem to be a reasonable approach, since it is expected that stronger collisions will be required to access higher lying electronic states. Using the statistical model discussed above, we find that the number of collisions above the surface is nearly zero for encounters with a collision radius of less than 1.1 Å. As this value is allowed to increase to 1.85 Å, the number of collisions is found to increase in approximately an exponential fashion. To assess the influence of particle velocity on the excitation probability we assume in a simple way that most of the closest encounters lead to population of the second excited state and the more distant encounters lead to population of the first excited state. For example, the contribution to each state might be

$$P_1 = P_1^0 \frac{(r-1.1)}{(1.85-1.1)} \tag{6}$$

and

$$P_2 = P_2^0 \frac{(r-1.85)}{(1.1-1.85)} \tag{7}$$

using a linear interpolation scheme.

The result of employing this approximation is shown in Figs. 6(c) and 6(d), where P_2^0 was chosen as a fitting parameter to be 0.19 and P_1^0 was kept at 0.76. As found previously[24] the ratio of the first excited state intensity to the ground state intensity has an exponential dependence at high velocity and is nearly independent of velocity at low velocities. The analogous ratio for the second excited state is independent of velocity for all velocities. Virtually identical results are obtained when employing different assumptions associated with picking appropriate values of the encounter distance. If we arbitrarily assume that the $a\ ^4F_{5/2}$ level is exclusively populated when the encounter distance is less than 1.7 Å and the $a\ ^4F_{7/2}$ state is populated when the encounter distance is greater than 1.7 Å but less than 1.85 Å, the same featureless type of velocity dependence is observed for the second excited state. Identical conclusions are also reached when analyzing data obtained at other polar angles of ejection.

It is interesting that physically realistic parameters can be found for this model which accurately reproduce the experimental data without involving the $\exp(-1/v_\perp)$ dependence seen for other conditions.[19,23,24] Although we are forced to speculate about this observation, it seems reasonable that this exponential behavior might dominate the velocity dependence at higher velocities, at values beyond our present experimental range. The characteristic decay times inside the solid are apparently much shorter for $a\ ^4F_{5/2}$ than for $a\ ^4F_{7/2}$.[34] This analysis certainly suggests then, that the unexpected experimental result, that the population of the $a\ ^4F_{9/2}$ level of Rh atoms desorbed from Rh {001} is nearly independent of velocity, may be explained as being associated with collisions over the surface.

IV. CONCLUSION

The energy-resolved angular distributions of Rh neutral atoms desorbed from ion bombarded Rh {001} have been measured for the ground ($a\ ^4F_{9/2}$) and the lowest two excited states ($a\ ^4F_{7/2}$,$a\ ^4F_{5/2}$). For a given kinetic energy the polar angle distributions show distinct variations with increasing excitation energy. As the excitation energy increases two pronounced effects have been observed (i) the dominant off-normal peak shifts toward the surface normal, and (ii) the minor peak occurring at the surface normal shows an increase in intensity. These observations suggest that there are complicated factors at work which are influencing the overall excitation probability.

Some of these complexities have been disentangled through an analysis of the energy and angle dependence of the population in both electronic states. Of special interest is that the ratio of the population in the $a\ ^4F_{9/2}$ state to the ground state of Rh exhibits almost no velocity dependence. This behavior has been shown to be characteristic of excitations which are created by two atoms which collide within a few angstroms over the crystal surface. Hence, the overall excitation probability consists of a mechanism with its roots in Hagstroms original ideas as well as a new mechanism which opens up due to the dynamical motion associated with the sputtering event itself.

These experiments and their associated theoretical explanations are far from complete. We need to learn more about the factors which control the coupling between atoms inside the solid and the electronic band states. Previous work has suggested, for example, that the configuration of the electronic state is important in determining the overall excitation probability.[35] In recent experiments we have found direct evidence for this effect by examining the ejection of Ni atoms from Ni{001}. For that system, there are two sets of overlapping manifolds with different electronic character which exhibit very different excitation probabilities.[36] There has been recent experimental evidence that collisional deactivation may further influence the distribution of electronic and molecular states of sputtered species.[37] In the future it will be necessary to take account of all of these mechanisms as well as other as yet undiscovered ones to provide a general understanding of this subject.

ACKNOWLEDGMENTS

The financial support of the National Science Foundation, the Office of Naval Research, the Department of Energy and the M. Sklodowska-Curie fund MEN/NSF-93-144 is gratefully acknowledged.

[1] N. Winograd and B. J. Garrison, in *Ion Spectroscopies for Surface Analysis*, edited by A. W. Czanderna and D. M. Hercules (Plenum, New York, 1991), pp. 45–142.
[2] B. J. Garrison, N. Winograd, D. M. Deaven, C. T. Reimann, D. Y. Lo, T. A. Tombrello, D. E. Harrison, Jr., and M. H. Shapiro, Phys. Rev. B **37**, 7197 (1988).
[3] W. Eckstein and M. Hou, Nucl. Instrum. Methods Phys. Res. B **31**, 386 (1988).
[4] R. Maboudian, Z. Postawa, M. El-Maazawi, B. J. Garrison, and N. Winograd, Phys. Rev. B **42**, 7311 (1990).
[5] W. Eckstein and M. Hou, Nucl. Instrum. Methods Phys. Res. B **53**, 270 (1991).
[6] A. Wucher, M. Watgen, C. Mössner, H. Oechsner, and B. J. Garrison, Nucl. Instrum. Methods Phys. Res. B **67**, 531 (1992).
[7] C. He, Z. Postawa, S. Rosencrance, R. Chatterjee, B. J. Garrison, and N. Winograd (unpublished).
[8] R. P. Webb and D. E. Harrison, Jr., Phys. Rev. Lett. B **50**, 1478 (1983).
[9] H. Feil, H. J. W. Zandvleit, M.-H. Tsai, J. D. Dow, and I. S. T. Tsong, Phys. Rev. Lett. **69**, 3076 (1992).
[10] H. J. W. Zandvliet, H. B. Elswijk, E. J. van Loenen, and I. S. T. Tsong, Phys. Rev. B **46**, 7581 (1992).
[11] R. Kelly, Phys. Rev. B **25**, 700 (1982).
[12] E. Veje, Phys. Rev. B **28**, 5029 (1983), and references cited therein.
[13] H. D. Hagstrum, Phys. Rev. **96**, 336 (1954).
[14] W. F. van der Weg and D. J. Bierman, Physica **44**, 206 (1969).
[15] C. W. White, D. L. Simms, N. H. Tolk, and D. V. McCaughan, Surf. Sci. **49**, 657 (1975).
[16] M. L. Yu, D. Grischkowsky, and A. C. Balant, Phys. Rev. Lett. **48**, 427 (1982).
[17] D. Grischkowsky, M. L. Yu, and A. C. Balant, Surf. Sci. **127**, 315 (1983).
[18] M. El-Maazawi, R. Maboudian, Z. Postawa, and N. Winograd, Phys. Rev. B **43**, 12 078 (1991).
[19] N. Winograd, M. El-Maazawi, R. Maboudian, Z. Postawa, D. N. Bernardo, and B. J. Garrison, J. Chem. Phys. **96**, 6314 (1992).
[20] J. J. Vrakking and A. Kroes, Surf. Sci. **84**, 153 (19797).
[21] M. H. Shapiro and J. Fine, Nucl. Instrum. Methods Phys. Res. B **44**, 43 (1989).
[22] M. H. Shapiro, T. A. Tombrello, and J. A. Fine, Nucl. Instrum. Methods Phys. Res. B **74**, 385 (1993).
[23] D. N. Bernardo, M. El-Maazawi, R. Maboudian, Z. Postawa, N. Winograd, and B. J. Garrison, J. Chem. Phys. **97**, 3846 (1992).
[24] D. N. Bernardo and B. J. Garrison, J. Chem. Phys. **97**, 6910 (1992).
[25] R. Bhatia and B. J. Garrison, J. Chem. Phys. **100**, 8437 (1994).
[26] M. L. Yu, Phys. Rev. Lett. **47**, 1325 (1981).
[27] M. L. Yu and N. D. Lang, Phys. Rev. Lett. **50**, 127 (1983).
[28] J.-H. Lin and B. J. Garrison, J. Vac. Sci. Technol. A **1**, 1205 (1983).
[29] C. E. Moore, *Atomic Energy Levels* (U. S. GPO, Washington, DC, 1971), Vol. 3, p. 29.
[30] R. Kelly, Nucl. Instrum. Methods Phys. Res. **194**, 583 (1982).
[31] P. H. Kobrin, G. A. Schick, J. P. Baxter, and N. Winograd, Rev. Sci. Instrum. **57**, 1354 (1986).
[32] D. W. Duquette and J. E. Lawler, J. Opt. Soc. Am. B **2**, 1948 (1985).
[33] G. S. Hurst, M. G. Payne, S. D. Kramer, and J. P. Young, Rev. Mod. Phys. **51**, 767 (1979).
[34] Reference 25 suggests that the lifetime of the $a\ ^4F_{7/2}$ state in the solid and near surface region is 5–8 fs.
[35] B. I. Craig, J. P. Baxter, J. Singh, G. A. Schick, P. H. Kobrin, B. J. Garrison, and N. Winograd, Phys. Rev. Lett. **57**, 1351 (1986).
[36] C. He and N. Winograd (unpublished).
[37] J. Fine, M. Szymonski, J. Kolodziej, M. Yoshitake, and K. Franzreb, Phys. Rev. Lett. **71**, 3585 (1993).